EPJ Web of Conferences **279**, 12001 (2023) https://doi.org/10.1051/epjconf/202327912001
NPA-X 2022

Nuclear level densities and γ-ray strength functions of ^{120,124}Sn for astrophysical purposes

Maria Markova[1,*], *Ann-Cecilie* Larsen[1], and *Frank Leonel* Bello Garrote[1]

[1]Department of Physics, University of Oslo, N-0316 Oslo, Norway

Abstract. The nuclear level densities (NLDs) and γ-ray strength functions (GSFs) of ^{120,124}Sn were extracted with the Oslo method, compared and combined with other experimental data to be used as inputs in the TALYS reaction code to constrain the Maxwellian-averaged cross sections (MACS) for the ^{119,123}Sn$(n,\gamma)^{120,124}$Sn reactions. For ^{120}Sn, the MACS are in relatively good agreement with the JINA REACLIB, BRUSLIB libraries, while no clear agreement was found for ^{124}Sn. In addition, the pygmy dipole resonance (PDR) was found to contribute with up to $\approx 3-8\%$ of the total MACS in these nuclei.

1 Introduction

Information on the neutron-capture cross sections and rates for nuclei in the vicinity of neutron rich stable and unstable Sn isotopes provides a deeper insight into the astrophysical s- and r-processes and abundances of elements produced in these processes in this mass region. In cases of unstable nuclei, any direct measurements of neutron-capture cross sections are greatly hindered and one has to exploit the potential of indirect techniques. The nuclear reaction codes, *e.g.* TALYS [1, 2], incorporate the Hauser-Feshbach framework [3], combining the statistical properties of nuclei, such as the nuclear level density (NLD) and γ-ray strength function (GSF), with other nuclear inputs to calculate the astrophysical values of interest. The NLD is given by the number of nuclear levels per excitation energy unit, while the GSF characterizes the reduced average γ-decay probability.

In cases of unstable neutron rich nuclei no experimental data on NLDs and GSFs are available, and constraining the neutron-capture cross sections and rates is limited by the set theoretical models, including microscopic calculations, available in TALYS as predefined calculation options. While the spread of theoretical NLDs can be considered somewhat small and the region of the giant dipole resonance is well-described by the available GSFs, the disagreement in low-lying dipole strengths below the neutron threshold is quite critical. Experimental data on the low-lying part of the $E1$ response, preferably obtained together with the NLDs, are highly desired in order to specify the constants on the neutron-capture cross sections. Gaining more knowledge on systematics of NLDs and GSFs in different isotopic chains will further facilitate estimating these cross sections indirectly for unstable, very neutron rich isotopes.

The Oslo method [5] is an experimental technique providing a simultaneous measurement of the GSF and NLDs in light charged particle induced reactions. In this work, we present

*e-mail: maria.markova@fys.uio.no

the NLDs (Sec. 2.1) and GSFs (Sec. 2.2) of ^{120,124}Sn used to experimentally constrain the Maxwellian-averaged cross sections (MACS) for the ^{119,123}Sn$(n,\gamma)^{120,124}$Sn reactions, presented in Section 3. Combining the Oslo $E1$ strength with the $E1$ and $M1$ GSFs deduced from spectra of relativistic Coulomb excitation in forward-angle inelastic proton scattering [4] provides an opportunity to study the contribution of the low-lying $E1$ strength, often referred to as the pygmy dipole resonance (PDR), to the total MACS. This study was performed for ^{120,124}Sn and will be discussed in Section 4.

2 The Oslo method

Both ^{120}Sn and ^{124}Sn nuclei were studied at the Oslo Cyclotron Laboratory (OCL) in the $(p, p'\gamma)$ reaction with 16 MeV protons. The setup at the OCL is presented by the γ-detector array OSCAR and the particle telescope SiRi (for more details see. [6]). OSCAR comprises of 30 large-volume $LaBr_3$(Ce) scintillator detectors fixed in a truncated icosahedron frame, surrounding the target chamber. The full-energy peak efficiency and energy resolution of OSCAR have been measured to be $\approx 20\%$ and $\approx 2.7\%$, respectively, at $E_\gamma \approx 662$ keV. The particle stripped telescope exploiting the $E - \Delta E$ technique is mounted in the backward position, cowering from 126° to 140°. Such form of the setup allows to collect p-γ coincidence events and, thus, the γ-spectra at each excitation energy of the nucleus below the neutron separation energy. These spectra are unfolded to correct for the detector response [6]. At the final stage of the coincidence event analysis, the first generation photons for each cascade at each excitation energy E_x are singled out to form a so-called primary matrix $P(E_x, E_\gamma)$. This matrix is the main input of the Oslo method providing a decomposition of the primary matrix into the transmission coefficient $\mathcal{T}(E_\gamma)$ and the NLD $\rho(E_x - E_\gamma)$ (for more details see [5, 6]):

$$P(E_x, E_\gamma) \propto \mathcal{T} \cdot \rho(E_x - E_\gamma), \tag{1}$$

where $\mathcal{T}(E_\gamma)$ is independent of the initial and final excitation energies according to the Brink-Axel hypothesis [5] and proportional to the GSF $f(E_\gamma)$ as $\mathcal{T}(E_\gamma) = 2\pi E_\gamma^{2L+1} f(E_\gamma)$. In the Oslo analysis it is assumed that the extracted GSF is predominantly of the dipole $L = 1$ nature.

This decomposition provides only the functional forms of the NLD and GSF and some additional experimental data are required to constrain the absolute values of these functions. The slope and the absolute value of the NLD are fixed with the discrete low-lying states and the value of the NLD at the neutron separation energy, obtained from the average s-wave neutron resonance spacing available from neutron resonance experiments. The GSF shares the same slope with the NLD and its absolute value is fixed with the total average radiative width obtained in the same neutron resonance experiments. All the details of the normalization procedure and parameters used are provided in [6] and the corresponding Supplementary Material.

2.1 Nuclear level densities of ^{120,124}Sn

The NLD of ^{120}Sn extracted with the Oslo method is shown in Fig. 1(a) together with the theoretical NLD provided as available options in TALYS. The total NLD of ^{124}Sn is very similar in slope and absolute value within the experimental error bands to ^{120}Sn and the previously published NLDs for other even-even ^{116,118,122}Sn isotopes (see [7] and references therein for further details). Indeed, no significant structural changes from ^{120}Sn to ^{124}Sn are expected to cause a noticeable difference in NLDs. Some minor differences in the slopes of NLDs for ^{120,124}Sn and the older data ^{116,118,122}Sn stem primarily from differences in the normalization procedure.

The NLDs for ^{120,124}Sn agree well with the low-lying discrete states [8] up to ≈ 3 MeV excitation energy, where the level scheme can be considered complete. Up to the neutron separation energy the NLDs demonstrate a rather smooth constant temperature behavior.

In order to crosscheck the normalization of the NLD in ^{124}Sn we compare a reduced Oslo NLD for $J = 1^-$ states with the corresponding NLD extracted with the fluctuation analysis of high resolution inelastic proton scattering spectra above 6 MeV [4]. The experimental data agree quite well within the error bars, however, demonstrate some disagreement with the TALYS input NLDs. As shown in Fig. 1(a) this difference might reach up to approximately a factor of 3. However, in general, the TALYS input NLDs follow the same trend as the experimental NLD and they are not expected to be the main source of TALYS uncertainty span for the MACS.

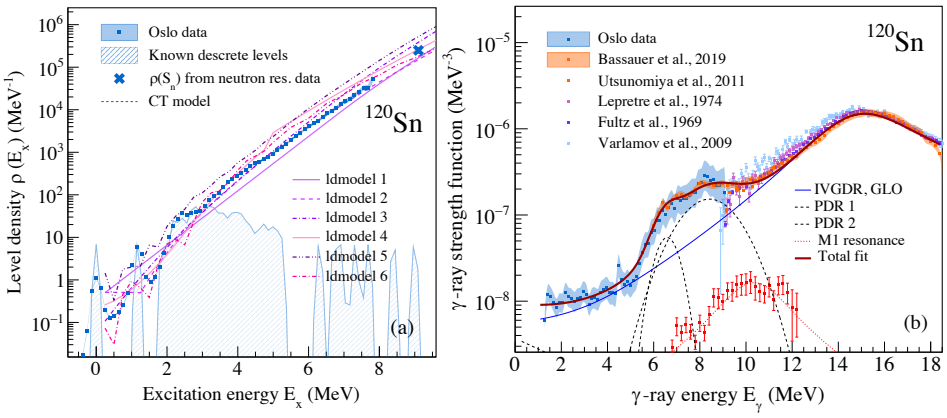

Figure 1. (a) The experimental NLD of ^{120}Sn shown with the discrete states from [8] and the theoretical NLD models available in TALYS. (b) The experimental GSF of ^{120}Sn shown together with the $E1$ and $M1$ strengths from Ref. [4] and (γ, n) experiments from Refs. [9–12]

.

2.2 γ-ray strength functions of ^{120,124}Sn

The GSFs of ^{120,124}Sn extracted with the Oslo method reach up to the neutron separation energy only and, therefore, need to be combined with the data above the neutron separation energy to present the total $E1 + M1$ response of the nucleus used for astrophysical calculations. The GSFs deduced from forward-angle inelastic proton scattering (p, p') at relativistic beam energies [4] have an overlap with the Oslo data between 6 MeV and the neutron separation energy. Combined with the Oslo data, it covers the whole γ-energy region of interest, including the low-lying part and the giant dipole resonance (GDR). Both data sets agree well within the error bands and reveal a double-peak structure below the neutron separation energy, often referred to as the PDR. The inelastic relativistic scattering experiment also provides the data on the $M1$ part of the response in both nuclei, which allows to perform the decomposition of the total $E1 + M1$ part of the response into the $M1$ part and the $E1$ part, comprising of the GDR and the PDR as a two-peak structure. The single and the generalized Lorentzian functions were used to parametrize the $M1$ and the GDR parts, respectively, while the PDR was best reproduced by two Gaussian peaks. Such a decomposition of different parts of the nuclear response for ^{120}Sn is shown in Fig. 1(b).

3 The MACS of ^{119,123}Sn(n, γ)^{120,124}Sn reactions

Both the experimental NLD and the GSF for each isotope were futher used as the inputs to calculate the MACS of ^{119,123}Sn$(n,\gamma)^{120,124}$Sn reactions with the TALYS code. The experimental MACS for both cases are shown in Fig. 2 together with the span of MACS obtained with all available calculation options in TALYS and the data from several commonly used libraries (see Fig. 2 caption for Refs.).

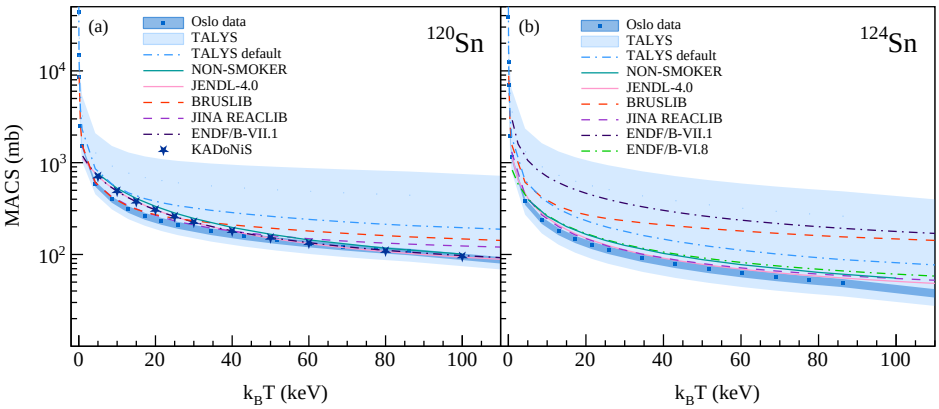

Figure 2. MACS of ^{119,123}Sn$(n,\gamma)^{120,124}$Sn reactions obtained with the Oslo method input NLDs and GSFs compared to the span of TALYS predictions (light blue band), NON-SMOKER [13], JENDL-4.0 [14], BRUSLIB [15], JINA REACLIB [16], ENDF/B-VII.1 [17], ENDF/B-VI.8 [18], KADoNiS [19] libraries.

,

For both ^{120}Sn and ^{124}Sn the experimental cross sections lie closer to the bottom part of the TALYS predictions. As the spread of the theoretical NLDs available in TALYS can be somewhat considered small, the main contribution to the TALYS uncertainty band is due to the spread of avalable TALYS GSFs, which poorly reproduce the experimental result. For the case of ^{120}Sn, the experimental MACS are in a fair agreement with the KADoNiS data point at 30 keV energy. For the energies below 30 keV, the cross section agrees quite well with the JINA-REACLIB and BRUSLIB data, while for higher energies it becomes closer to the ENDF/B-VII.1 and JENDL-4.0 cross sections. For ^{124}Sn the data from different libraries disagree with each other and the experimental cross section. JINA-REACLIB and JENDL-4.0 data agree the best with the experimental error band along the whole shown energy range. The spread of predictions from libraries is significantly larger than for ^{120}Sn, which might be expected for the radiative neutron capture reaction on an unstable ^{123}Sn target.

4 The role of the pygmy dipole resonance

As the combination of the Oslo and the (p, p') data allows for the decomposition of the total nuclear response into the $E1$ and $M1$ components, it becomes possible to study the astrophysical role of the low-lying dipole strength, namely the PDR. The MACS were calculated with the total $E1$ response, comprising of the GDR and two peaks of the PDR, and with the $E1$ response presented by GDR only. These results are shown together with the TALYS uncertainty span in Fig. 3. The fraction of the energy weighted sum rule for dipole transitions

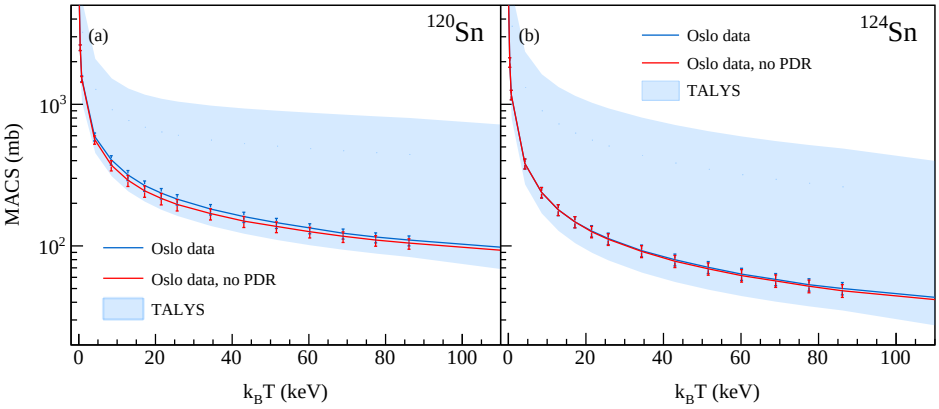

Figure 3. The MACS of ^{119,123}Sn$(n,\gamma)^{120,124}$Sn reactions obtained with and without the PDR part of the total $E1$ response compared with the TALYS span of cross sections.

exhausted by the PDR is ≈3% in ^{120}Sn and ≈2% in ^{124}Sn. For the largest PDR in ^{120}Sn, its contribution to the total MACS reaches up to ≈8%, while for the smallest PDR in ^{124}Sn it reaches up to ≈3%. Even though these contributions for stable ^{120,124}Sn are quite moderate, for the neutron rich experimentally studied ^{130}Sn [20] with the PDR of ≈ 7% we might expect this contribution to be larger that ≈ 10% of the total MACS.

5 Conclusions

The experimental NLDs and GSFs of ^{120,124}Sn were extracted with the Oslo method and combined with the relativistic inelastic proton scattering data to experimentally constrain the radisative neutron capture ^{119,123}Sn$(n,\gamma)^{120,124}$Sn MACS with the reaction code TALYS. The spread of available theoretical $E1$ GSFs in TALYS contributes to a large span of TALYS calculations. The experimental constrains narrow down the spread of MACS significantly as compared to the theoretical models. The MACS calculated for ^{120}Sn were found to be in good agreement with JINA REACLIB, BRUSLIB libraries, while no clear agreement is seen in ^{124}Sn. The pygmy dipole resonances in ^{120,124}Sn were found to contribute with up to ≈ 3 – 8% of the total MACS. For the heavier neutron rich Sn isotopes this contribution might be expected to be quite significant, and, therefore, to be of importance for reproducing solar system abundances of elements produced in the r-process.

References

[1] A. Koning, S. Goriely, and S. Hilaire, TALYS-1.9, A nuclear reaction program, user manual, Tech. Rep. (2017).
[2] A. Koning, *et al.*, Nuclear Data Sheets 155, 1 (2019).
[3] W. Hauser and H. Feshbach, Phys. Rev. 87, 366 (1952).
[4] S. Bassauer, *et al.*, Phys. Rev. C 102, 034327 (2020).
[5] A. C. Larsen, *et al.*, Phys. Rev. C 83, 034315 (2011).
[6] M. Markova, *et al.*, Phys. Rev. Lett. 127, 182501 (2021).
[7] M. Markova, *et al.*, to be published (2022).

[8] Data taken from the ENSDF database of the NNDC online data service, https://www.nndc.bnl.gov/ensdf/. Last accessed: January 19, 2022.
[9] H. Utsunomiya, S. Goriely, M. Kamata, *et. al.*, Phys. Rev. C 84, 055805 (2011).
[10] V. V. Varlamov, *et al.*, Bull. Rus. Acad. Sci. 74, 833 (2010).
[11] A.Leprêtre, *et.al.*, Nucl. Phys. A 219, 39 (1974).
[12] S. C. Fultz *et.al.*, Phys. Rev. 186, 1255 (1969).
[13] T. Rauscher and F. K. Thielemann, At. Data Nucl. Data Tables **75**, 1 (2000).
[14] K. Shibata, *et al.*, J. Nucl. Sci. Technol. **48(1)**, 1-30 (2011)
[15] Y. Xu, *et al.* , A&A **549**, A106 (2013).
[16] R. H. Cyburt, *et al.*, Astrophys. J., Suppl. Ser. **189**, 240 (2010).
[17] M. B. Chadwick, *et al.*, Nucl. Data Sheets **112**, 2887-2996 (2011).
[18] H. D. Lemmel, *et al.*, IAEA-NDS-100, Rev. **11** 1-32 (2001).
[19] Data extracted using the KADoNiS On-Line Data Service, http://www.kadonis.org, accessed 2022-08-05.
[20] P. Adrich, *et. al*, Phys. Rev. Lett. 95, 132501 (2005).